Academic Science Journal

Synthesis of LiCo0.25Ni0.75O2 via Citric-urea Combustion Route as a Cathode for Lithium-ion Batteries

H. T. Homad[*1], O. A. Al-Jubouri [1], Noor M. Ali[2], M. H. AL-TIMIMI[2]

[1]General Directorate of Education, Diyala

[2]Department of Physics, College of Science, University of Diyala

alhudaa613@gmail.com

Received: 24 April 2024 **Accepted: 11 June 2024**

Published: October 2025

DOI: https://dx.doi.org/10.24237/ASJ.03.04.874D

Abstract

The $LiCo_{0.25}Ni_{0.75}O_2$ compound was prepared as a cathode active material for lithium–ion batteries by a citric-urea combustion rout in this study. The study presented a comprehensive analysis of the decomposition process and formation of metal oxides in $LiCo_{0.25}Ni_{0.75}O_2$ sample using Thermogravimetric Analysis (TGA), crystalline structure and surface morphology of the prepared powder are investigated by (XRD) and (FESEM). In this study, the electrochemical performance of the a cathode material prepared using different techniques was examined, including cyclic voltammetry, electrochemical impedance spectroscopy, and measuring the initial charge and discharge capacities along with the capacity retention. The results of the XRD patterns for $LiCo_{0.25}Ni_{0.75}O_2$ sample shows high intensity peaks that indicated a good crystallinity with the Calcination Temperature, while the morphology findings indicate that the sample was within nanostructured dimensions. Electrochemical measurements showed. The capacity of the charging and discharging were of 177.6 $mAhg^{-1}$ and 166.9 $mAhg^{-1}$ delivered by the $LiCo_{0.25}Ni_{0.75}O_2$ cathode. Likewise, a columbic efficiency of 93.9% was obtained for the cathode.

Keywords: Lithium-ion batteries; citric-urea combustion route; cathode material; TGA; Electrochemical Characterization.

Introduction

Energy production and storage have become a significant concern in recent times due to the continuing depletion of fossil fuels such as coal, oil, and gas, which are predicted to run out by 2090. To meet the present energy demand, we must thus discover other energy sources [1,2].

Energy storage batteries are among the most important storage technologies, due to their long cycle life and high energy density. In case of an emergency, batteries may be used as a chemical energy storage source [3].

Since lithium-ion batteries offer such high energy, power density, stability, and dependability, they have long been regarded as an effective energy storage solution. Over the past several decades, Lithium-ion batteries (LIBs) have taken centre stage in many fields of research. In addition to being widely used in portable electronics, lithium-ion batteries are also expected to be a major component of smart power grids and electric car technology [4,5].

The de-intercalation of lithium ions anf the reversible intercalation that occur between anode and cathode is the basis for their operation [6–8]. The main performance attributes of batteries, high energy, high voltage, high speed charging, good safety, and better stability improved power grids, automobiles and drones [9–12]. This has led to a great deal of study in the field of nanotechnology materials for electrodes in an effort to maximise ion storage operations at the nanoscale and push the limits of lithium-ion batteries. The development of high-performance cathode materials is especially crucial because the cathode directly influences electrochemical properties that are essential to the efficient operation of modern lithium-ion batteries, included specific capacity, voltage of operation, cycle stability [13–15].

Generally speaking, the quickest approach to enhance the electrochemical performance of Lithium-ion batteries (LIBs) is to locate the best cathode material combination by creating preparation techniques with various parameters to manage the cathode architectures and crystallisation degrees [16]. This work effectively synthesised layered $LiCo_{0.25}Ni_{0.75}O_2$ cathodes using a new citric-urea self-combustion method. Batteries provide numerous benefits to society, including energy storage, portable devices, renewable energy integration, electric

vehicles, medical applications, and energy independence. Overall, batteries are crucial for technological advancement, improving quality of life, and promoting environmental sustainability.

Experimental Details

$LiCo_{0.25}Ni_{0.75}O_2$ Nanoparticles were produced by using of the citric-urea combustion rout. Stoichiometric molar amounts were weighed in accordance with their molecular weights in order to create the sample. The following equation was used to get the reactant weights:

Mass (g) = No. of moles × Molar Mass (g/mol) (1)

$LiCo_{0.25}Ni_{0.75}O_2$ sample preparation involved first weighing and completely dissolving the materials (LiCl, $CoCl_2.6H_2O$, $NiCl_2.6H_2O$) in distilled water, then mixing the mixture while stirring continuously. Next, an aqueous solution of urea ($NH_2.CO.NH_2$) and citric acid ($C_6H_8O_7$) was added to the first solution with mixing to form the starting solution (100 ml), in which the molar ratio of citric acid to metal ions is (1:2) and the molar ratio of urea to metal ions is (1:1). Ultimately, HNO_3 are mixed at a volume ratio of 1:0.1 with the starting solution while being continuously stirred. The resultant solutions underwent continuous stirring for four hours at a temperature of 85 °C to facilitate water evaporation. Up until dark blue gel was produced, the solution's viscosity was steadily raised while dark blue resin was formed and intermittent foaming was seen. The resultant resin was cured for six hours at 180 °C. After the gel's volume was increased three or four times above its starting volume, an intermediate compound known as polymeric intermediate was created. Additionally, it was calcined for four hours at temperature of 800°C [15].

Results and Discussions

1. Thermal Gravimatric Analysis (TGA)

The TGA diagram of $LiCo_{0.25}Ni_{0.75}O_2$, which was synthesized using the citric-urea combustion rout, is depicted in Figure 1. The $LiCo_{0.25}Ni_{0.75}O_2$ sample, synthesized by the citric-urea combustion rout, undergoes four decomposition stages with a total weight loss of 56.02%. The stages are as follows: 5.99% weight loss at 40-160°C (likely from water loss), 8.99% weight

loss at 160-285°C (possibly from organic decomposition), a significant 28.55% weight loss at 285-475°C (likely from further organic decomposition and metal oxide formation), and 12.49% weight loss at 475 - 740°C (possibly from further metal oxide transformations) [17,18]. Table1 lists both temperature zones and loss weight of the prepared $LiCo_{0.25}Ni_{0.75}O_2$ sample.

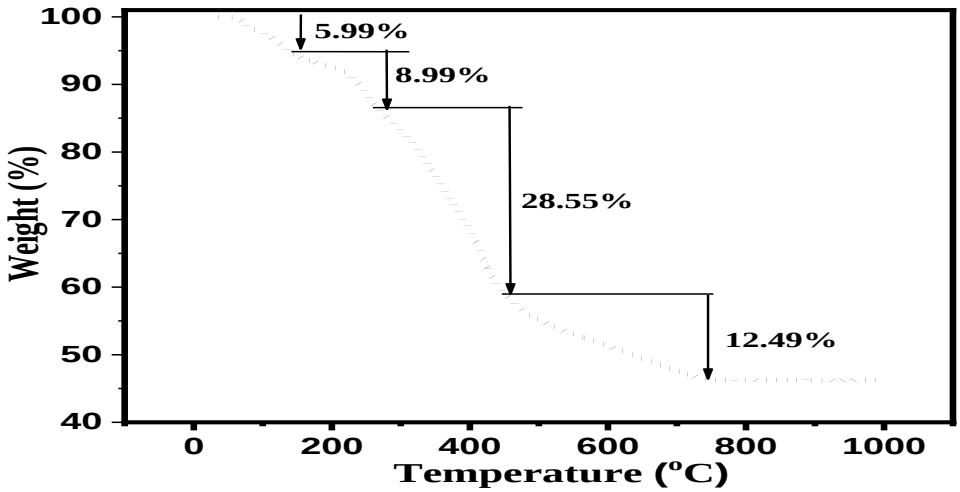

Figure 1: The TGA diagram for $LiCo_{0.25}Ni_{0.75}O_2$ sample.

Table 1: The TGA results of $LiCo_{0.25}Ni_{0.75}O_2$ sample

Sample	synthesis method	Region of Decomposition	Temperature Range (°C)		Weight Loss (%)	
			Start	End	Partial	Total
$LiCo_{0.25}Ni_{0.75}O_2$	citric-urea combustion rout	1st	40	160	5.99%	56.02%
		2nd	160	285	8.99%	
		3rd	285	475	28.55%	
		4th	475	<800	12.49%	

2. X-ray Diffraction (XRD)

The structure and the phases of $LiCo_{0.25}Ni_{0.75}O2$ powder have been determined by X-Ray Diffraction analysis. The characteristic peaks at (2Θ= 37.82°, 43.93°, 44.99°, 63.92°, 65.07°, 76.73° and 79.8°) of the planes (111), (002), (104), (022), (018), (113) and (222) respectively, indicates the formation of cubic $LiNiO_2$ nanostructure of space group (Fm-3m no. 225), which well agreed with (JCPDS 98-002-9236) and (JCPDS 98-01-4801), as shown in figure (2). The

crystalline size of $LiCo_{0.25}Ni_{0.75}O2$ powder was calculated by Scherrers equation (eq.2) [19], to be 38.49 nm).

$$\mathbf{D = 0.9\ \lambda / (\beta \cos\theta)} \quad (2)$$

Where D is the crystallite size, λ is the X-ray wavelength, β is the full width athalf maximum (FWHM) and θ is the Bragg's angle.

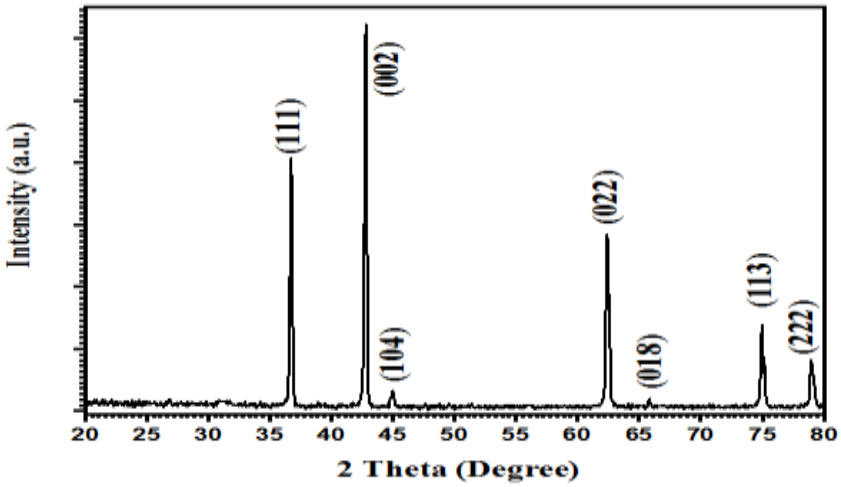

Figure 2: XRD pattern of ($LiCo_{0.25}Ni_{0.75}O2$) sample.

3. Field-Emission Scanning Electron Microscopy:

The morphology and particle size distributions histogram of $LiCo_{0.25}Ni_{0.75}O_2$ sample were described using FESEM images. As shown in Figure 3a,b, The images show that the sample is well-formed polycrystalline materials. The majority of the crystals in all the materials are polyhedrals. It seemed that a few of the crystals were modestly aggregating into larger particles [20].

Academic Science Journal

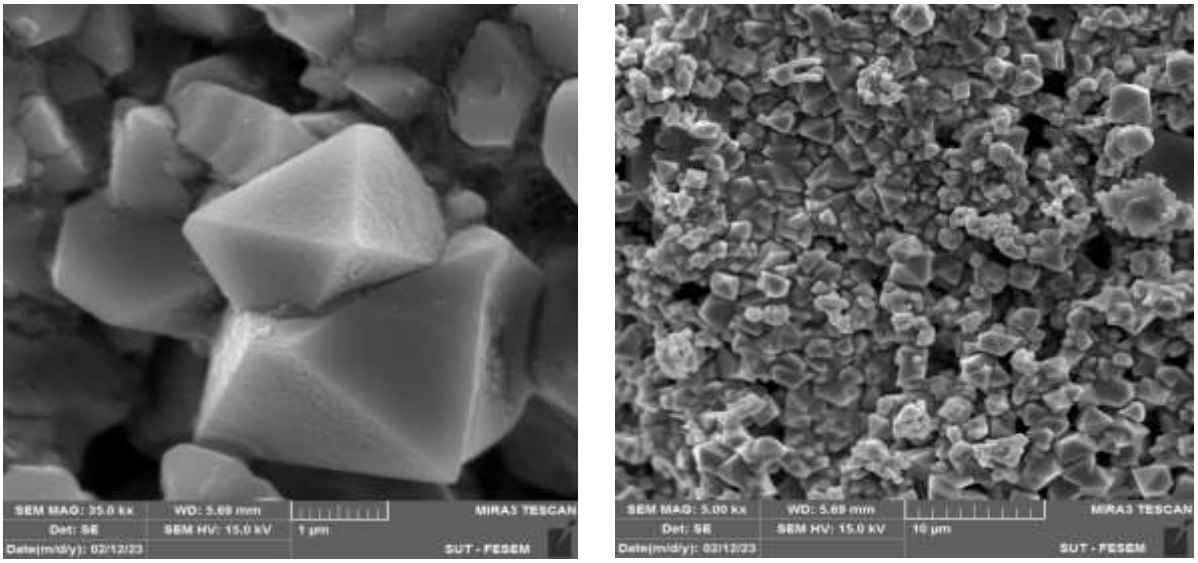

(a)

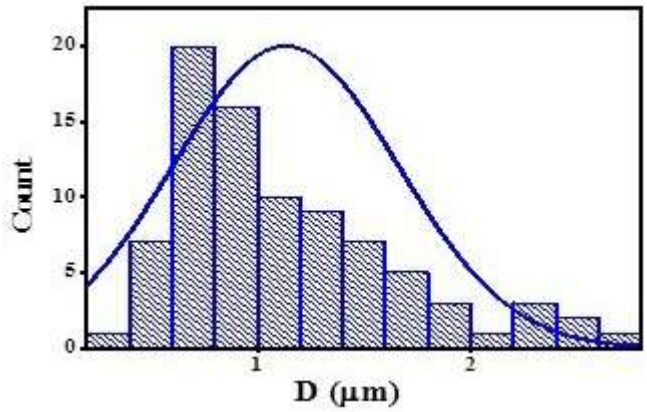

(b)

Figure 3: a- FESEM images for LiCo0.25Ni0.75O2 at various magnification levels.

b- Histograms depicting particle size distributions

4. Electrochemical Characterization

- **Cyclic voltammetry (CV)**

Figure 1 demonstrates the cyclic voltammograms of the cathode material of $LiCo_{0.25}Ni_{0.75}O_2$. The CV diagrams were obtained using Potentiostat/Galvanostat Autolab at a scan rate of 0.1 mV s^{-1} in the potential ranging from 2.5 to 4.5 V. A sharp oxidation peak is detected at ~3.9 V

and a broad reduction peak at ~3.7 V, which are attributed to the insertion/extraction of lithium ions within the electrode. In addition, an attenuated oxidation peak approximately located at 4.2 V and also a weak reduction peak situated at ~4.0 V are found in the CV curve of the cathode material**.** In the $LiCo_{0.25}Ni_{0.75}O_2$ cathode material, the operating voltage is ascribed to the Fermi energy level of the electrons of 3d orbital, which varies as CoO2 (3d5/3d6) > NiO2 (3d6/3d7). If the Ni^{+3} ions in the cathode are mainly associated with intercalation/de-intercalation of the lithium ions, the redox peaks located at higher potential can be imputed to the contribution of Co^{+3} ions in the redox reaction, since Co^{+3}/Co^{+4} appears at a higher potential than that of Ni^{+3}/Ni^{+4}. Accordingly, the oxidation and reduction peaks respectively at 4.2 and 4.0 V are associated with the Co^{+3}/Co^{+4} redox reaction [21].

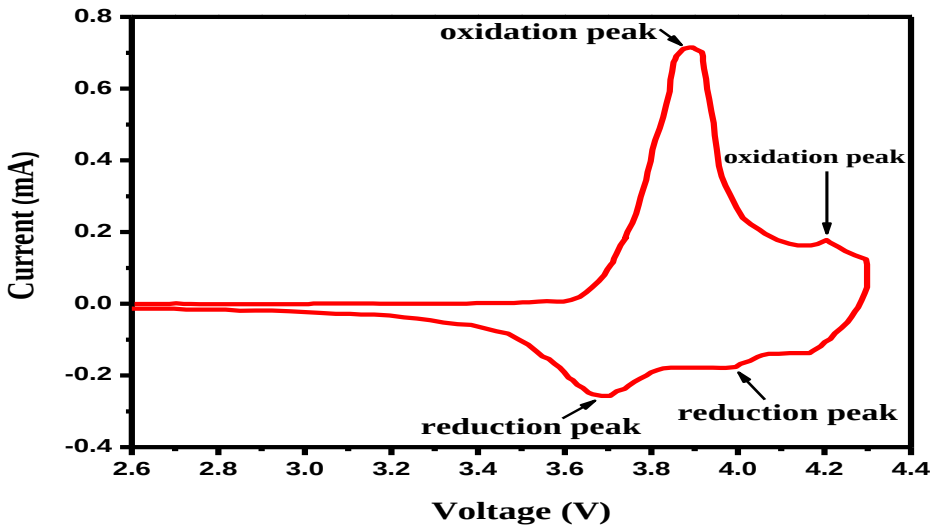

Figure 4: The CV curve of LiCo0.25Ni0.75O2 recorded at a scan rate of 0.1 mV s^{-1} in the voltage range of 2.5 to 4.5 V

- **Electrochemical impedance spectroscopy (EIS)**

Figure 5 demonstrates the electrochemical impedance spectroscopy (EIS) curves of the $LiCo_{0.25}Ni_{0.75}O_2$ cathode material. The equivalent circuit shown in Figure 5 2 was used for the fitting of the Nyquist plots. The Nyquist diagrams of the cathode material shown in Figure 5

comprise of a semicircle found at medium-to-low frequency along with a straight slope line detected at low frequency. The intersection point of the Nyquist plots and the Z_{re}' axis at high frequency is relevant to the electrolyte bulk resistance (R_s), which signifies the ionic conductivity of the electrolyte. The semicircular changing from the medium to low frequency is pertinent to the charge transfer resistance (R_{ct}) between the cathode and electrolyte and also the kinetic of the electrochemical reactions occurred in the positive electrode. The straight slope line defined as the Warburg impedance (W_0) corresponds to the diffusion of Li^+ ions within the bulk of the cathode material [22-24]. According to the results, the $LiCo_{0.25}Ni_{0.75}O_2$ cathode material exhibited an electrolyte bulk resistance of 2.6 Ω, a charge transfer resistance of 49.14 Ω, and a Warburg impedance of 0.051 Ω.

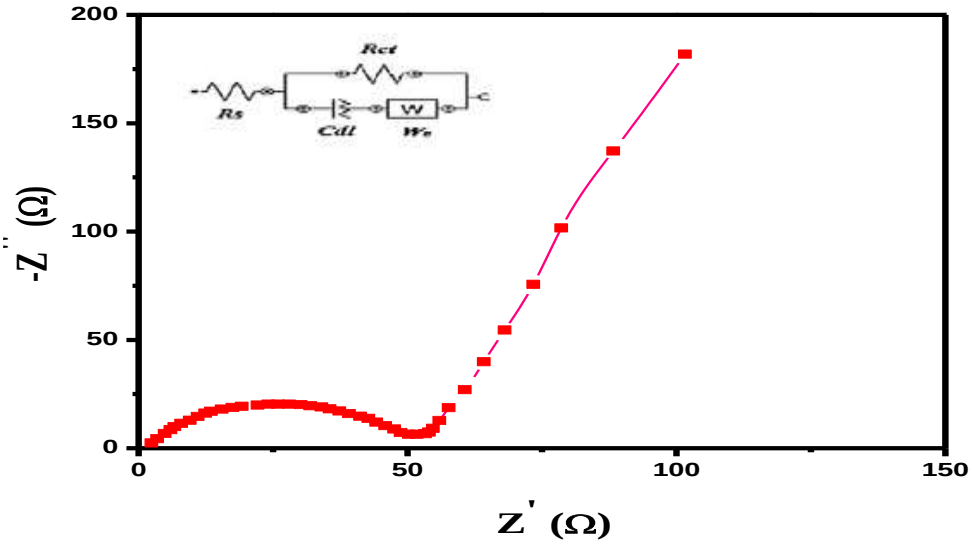

Figure 5: The Nyquist plots of the $LiCo_{0.25}Ni_{0.75}O_2$ electrode and the equivalent circuit hired for the fitting of the EIS curves

- **Charge and discharge cycles**

The initial charge and discharge cycles of the half-cells of the $LiCo_{0.25}Ni_{0.75}O_2$ cathode material as the working electrode and the lithium foil as the counter electrode. The measurements were done in the voltage (2.5-4.5) V at 0.1C using a battery tester. The results reveals that

$LiCo_{0.25}Ni_{0.75}O_2$ cathode delivered a charge capacity of 177.6 mAh/g and a discharge capacity of 166.9 mAh/g, corresponding to a Coulombic efficiency of 93.9%.

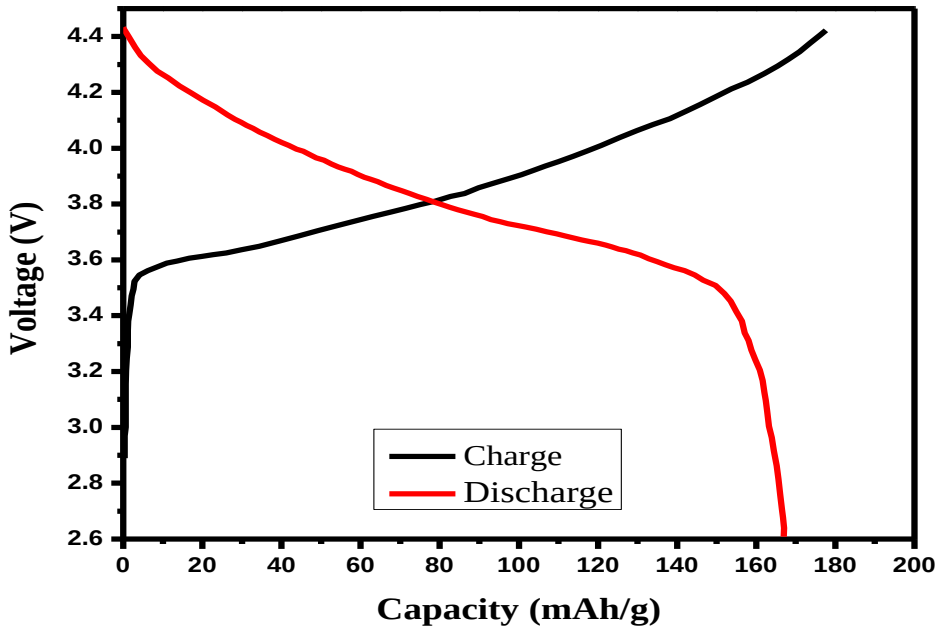

Figure 6: The first charge and discharge cycle of half-cells where $LiCo_{0.25}Ni_{0.75}O_2$ was assigned as the working lithium and electrode was used as the counter electrode

- **Stability percentage**

The capacity retention versus the cycle number curves of the $LiCo_{0.25}Ni_{0.75}O_2$ electrode material is appeared in Figure 7. The cyclic performance of the electrodes was examined using a battery tester, a voltage of 2.5 to 4.5 V and a C-rate of 0.1. The $LiCo_{0.25}Ni_{0.75}O_2$ electrode material showed delivered a capacity retention of 92.1%.

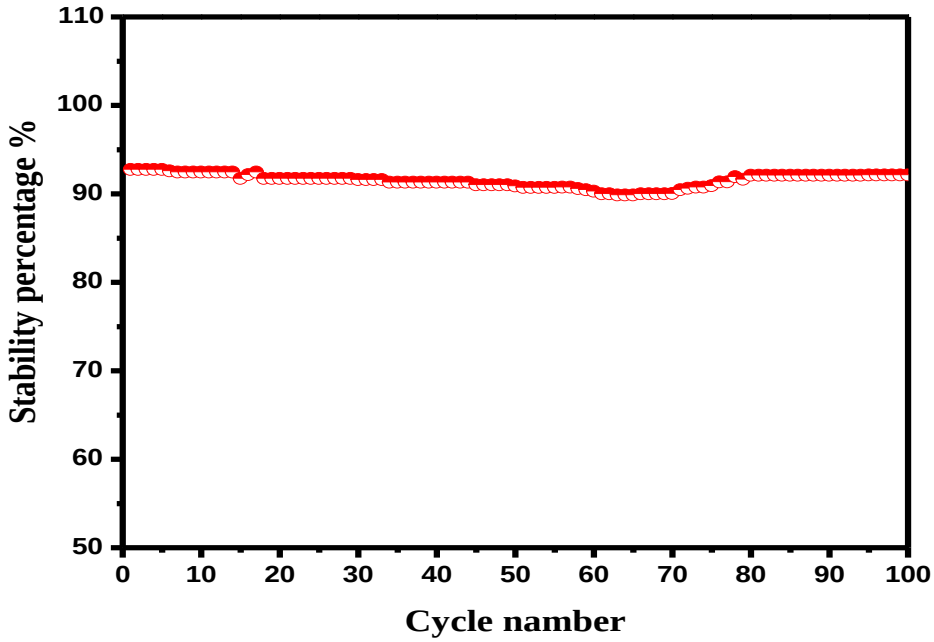

Figure 7: The stability percentage versus the cycle number of $LiCo_{0.25}Ni_{0.75}O_2$ electrode material after 100 cycles in the voltage ranged (2.5-4.5) V and the C-rate of 0.1.

Conclusions

The citric-urea combustion rout was used to successfully synthesize $LiCo_{0.25}Ni_{0.75}O_2$ for lithium–ion battery cathode. The citric-urea combustion rout led to a total weight loss of up to 56.02%. Suggesting a more complete decomposition and formation of metal oxides. This could have been attributed to the citric-urea combustion rout's higher efficiency in decomposing organic components and forming metal oxides. The composition and structure of these materials have been investigated; XRD pattern shows the formation of cubic $LiNiO_2$ nanostructure and confirms that all the peaks are very sharp, indicating a high crystallinity of the powder. The electrochemical performance was assessed using techniques like cyclic voltammetry and electrochemical impedance spectroscopy. The preparation method of electrode materials crucially influences their structure and surface characteristics, enhancing conductivity and structural stability, and leading to improved charge retention.

Source of funding: Source of funding: This research received no funding from any agency.

Conflict of interest: The authors declare that there is no conflict of interest.

Ethical clearance: Ethical approval was not required for this study.

References

[1] B. Dunn, H. Kamath, J. M. Tarascon, Electrical energy storage for the grid: a battery of choices, Science, 334(6058), 928-935(2011), DOI(https://doi.org/10.1126/science.1212741)

[2] M. Z. Abdullah, H. M. Hasan, M. H. Al-Timimi, W. H. Albanda, M. K. Alhussainy, Preparation and characterization of carbon doped lithium iron phosphate composite as cathode for rechargable battery, Journal of Ovonic Research, 15(3), (2019)

[3] Z. Šimić, D. Topić, G. Knežević, D. Pelin, Battery energy storage technologies overview, International journal of electrical and computer engineering systems, 12(1), 53-65(2021), DOI(https://doi.org/10.32985/ijeces.12.1.6)

[4] J. B. Goodenough, and K. S. Park, The Li-Ion Rechargeable Battery: A Perspective, American Chemical Society, 135(4), 1167-1176(2013), DOI(https://doi.org/10.1021/ja3091438)

[5] J. Xu, X. Cai, S. Cai, Y. Shao, C. Hu, S. Lu, and S. Ding, High-Energy Lithium-Ion Batteries: Recent Progress and a Promising Future in Applications, Energy &Environmental Materials, 6, 2575-0356(2023), DOI(https://doi.org/10.1002/eem2.12450)

[6] B. Ren, H. Cui, and C. Wang, Self-supported graphene nanosheet-based composites as binder-free electrodes for advanced electrochemical energy conversion and storage, Electrochem Energy Rev, 5(32), (2022), DOI(https://doi.org/10.1007/s41918-022-00138-6)

[7] A. Haider, R. Al-Anbari, G. Kadhim, and Z. Jameel, Synthesis and photocatalytic activity for TiO 2 nanoparticles as air purification, MATEC Web Conf, 162, (2018), DOI(https://doi.org/10.1051/matecconf/201816205006)

[8] M. Z. Abdullah, H. M. Hasan, M. H. Al-Timimi, W. H. Albanda, M. K. Alhussainy, M. Dumitru, Journal of Ovonic Research, 15(3), 199-204(2019)

[9] A. G. Olabi, Q. Abbas, P. A. Shinde, and M. A. Abdelkareem, Rechargeable batteries: technological advancement, challenges, current and emerging applications, Energy, 266, 126408(2023), DOI(https://doi.org/10.1016/j.energy.2022.126408)

[10] M. Akhilash, P. S. Salini, B. John, and T. D. Mercy, A journey through layered cathode materials for lithium ion cells – from lithium cobalt oxide to lithium-rich transition metal oxides, J. Alloys Compd, 869, 159239(2021), DOI(https://doi.org/10.1016/j.jallcom.2021.159239)

[11] S. S. H. Al-Mgrs, M. H. A. Al-Timimi, M. Z. Abdullah, and W. H. Al-Banda, Structural and optical characterizations of synthesized CMC/PVP-SnO2 nano composites, AIP Conference Proceedings, 2475(1), (2023), DOI(https://doi.org/10.1063/5.0102768)

[12] J. H. Adawiya, K. M. Chahrour , A. J. Addie, A. Q. Abdullah, P. R. Jubu, S. I. AL-Saedi, and A. N. Naje, Crystallinity tuning of LCNO/graphene nanocomposite cathode for high-performance lithium-ion batteries, Materials Science and Engineering B, 300, 117116(2024), DOI(https://doi.org/10.1016/j.mseb.2023.117116)

[13] A. J. Haider, R. A. Rsool, M. J. Haider, R. A. Rsool, and A. B. Dheyab, Properties of LiCo0.5Ni0.45Ag0.05O2 thin films for high storage energy capacity by pulsed laser deposition, Energy Rep, 6, 85–94(2020), DOI(https://doi.org/10.1016/j.egyr.2020.08.028)

[14] X. Cui, L. Zhang, Y. Hu, D. Yang, and J. Zou, Optimization of VOSO4@C cathode materials with CNT and GO for lithium-ion batteries, J. Alloys Compd., 914, 165354(2022), DOI(https://doi.org/10.1016/j.jallcom.2022.165354)

[15] M. S. Shalaby, M. O. Alziyadi, H. Gamal, and S. Hamdy, Solid-state lithium-ion battery: the key components enhance the performance and efficiency of anode, cathode, and solid electrolytes, J. Alloys Compd, 969, 172318(2023), DOI(https://doi.org/10.1016/j.jallcom.2023.172318)

[16] M. Z. Abdullah, M. H Al-Timimi, W. H. Albanda, M. Dumitru, A. E. Balan, C. Ceaus, and I. Stamatin, Structural and Electrochemical Properties of P3-Na0. 67Mn0. 3Co0. 7O2 Nanostructures Prepared by Citric-Urea Self-Combustion Route as Cathode for Sodium Ion Battery, Digest Journal of Nanomaterials and Biostructures, 4, 1179-1193(2019)

[17] N. Balasooriya, and P. Bandaranayake, Electrochemical Properties of $LiCo_{0.4}Ni_{0.6}O_2$ and its Performances in Rechargeable Lithium Batteries, Sri Lankan Journal of Physics, 8, (2007), DOI(https://doi.org/10.4038/sljp.v8i0.213)

[18] P. Periasamy, B. R. Babu, R.Thirunakaran, and N.Kalaiselvi, Solid-state synthesis and characterization of $LiCoO_2$ and $LiNi_yCo_{1-y}O_2$ solid solutions, Bulletin of Materials Science, 23(5), (2000), DOI(https://doi.org/10.1007/BF02708382)

[19] K. S. Landage, G. K Arbade, P. Khanna, C. J Bhongale, Biological approach to synthesize TiO2 nanoparticles using *Staphylococcus aureus* for antibacterial and anti-biofilm applications, Journal of Microbiology & Experimentation, 8, 36 - 43(2020), DOI(https://doi.org/10.15406/jmen.2020.08.00283)

[20] S. S. Nisa, M. Rahmawati, C. S. Yudha, H. Nilasary, H. Nursukatmo, H. S. Oktaviano, S. U. Muzayanha, and A. Purwanto, A Fast Approach to Obtain Layered Transition-Metal Cathode, Batteries, Material for Rechargeable Batteries, 8(4), (2022), DOI(https://doi.org/10.3390/batteries8010004)

[21] Y. Chen, G.X. Wang, J. P. Tian, K. Konstantinov, and H. K. Liu, Preparation and properties of spherical $LiNi_{0.75}Co0_{.25}O_2$ as a cathode for lithium-ion batteries, Electrochimica acta, 50, 435-441(2004), DOI(https://doi.org/10.1016/j.electacta.2004.03.053)

[22] T. F. Yi, Z. K. Fang, Y. Xie, Y.R. Zhu, and L.Y. Zang, Synthesis of $LiNi_{0.5}Mn_{1.5}O_4$ cathode with excellent fast charge-discharge performance for lithium-ion battery, Electrochimica acta, 147, 250-256(2014), DOI(https://doi.org/10.1016/j.electacta.2014.09.119)

[23] D. Li. Luo, G. Fu, C. Zheng, J. Fan, J. Q. Li, and L. Li, A New Spinel-Layered Li-Rich Microsphere As A High-Rate Cathode Material For Li-Ion Batteries, Advanced energy materials, 4(11), 1400062(2014), DOI(https://doi.org/10.1002/aenm.201400062)

[24] C. Deng, S. Zhang, S. Y. Yang, Y. Gao, B. Wu, L. Ma, B. L. Fu, Q. Wu, and F. L. Liu, Effects of Ti and Mg codoping on the electrochemical performance of $Li_3V_2(PO_4)_3$ cathode material for lithium ion batteries, The Journal of Physical Chemistry C, 115(30), 15048-15056(2011), DOI(https://doi.org/10.1021/jp201686g)